

Validation of TRMM PR rainfall over Brazil.

by

Sergio H. Franchito, V. Brahmananda Rao, Ana C. Vasques, Clovis M. E. Santo,

and Jorge C. Conforte

Centro de Previsão de Tempo e Estudos Climáticos, CPTEC

Instituto Nacional de Pesquisas Espaciais, INPE

CP 515, 12245-970, São José dos Campos, SP, Brazil

## Abstract

In an attempt to validate TRMM PR over Brazil TRMM PR estimates are compared with rain gauge station data from ANEEL and combined satellite/station data from GPCP. The results showed that TRMM PR seasonal rainfall is well correlated with ANEEL rainfall (c.c significant at 99% confidence level) over most of Brazil. The random and systematic errors are sensitive to seasonal and regional differences. During DJF and MAM TRMM PR rainfall is reliable over Brazil. In JJA (SON) TRMM PR estimates are only reliable in the Amazonian and southern (Amazonian and southeastern) regions. In general the seasonal regional characteristics of rainfall over Brazil are qualitatively well reproduced by TRMM PR and GPCP. The precipitation in TRMM PR is less than in GPCP over most of Brazil during DJF. The highest negative differences TRMM PR minus GPCP are found in the northeastern Amazonia and in the central Brazil. The negative differences between TRMM PR and GPCP rainfall are due to the overestimation of convective rainfall by IR and OLR sensors in GPCP. Over the southern region TRMM PR estimates exceed ANEEL and GPCP rainfall during JJA. Although TRMM PR is reliable in this region in JJA, the % rmse is higher in TRMM PR than in GPCP. In general, for most seasons TRMM PR is more reliable than GPCP over the regions with sparse data coverage, such as the Amazonia and central Brazil, while the use of GPCP is more adequate where there is a dense rain gauge network, such as the northeastern and southern regions.

## 1. Introduction

Seasonal and interannual climate variability in tropics is mainly determined by the precipitation variability. Brazil is a vast country of continental dimensions with various regimes of precipitation. The northwest of the Amazon basin is characterized by high precipitation rates (or order of 3000 mm yr<sup>-1</sup>); abundant rain occurs along the coastline of the easternmost part of Brazil (2000 mm yr<sup>-1</sup>), while some parts of the northeast region receives meagre precipitation, including the region known as the “drought polygon”, where the annual precipitation can be lower than 400 mm yr<sup>-1</sup>. The prevailing regimes in the southern and southeastern Brazil exhibit a large spatial variability. Precipitation in Brazil also shows a temporal variability, with different rainy seasons for different regions (Rao et al., 1996). These general characteristics are well documented in various text books on Climatology (Trewartha et al., 1961; Ratisbona, 1976, Hastenrath, 1991, among others).

Precipitation variability has a great impact on agricultural productivity and water and energy resources. A better knowledge of climate and climate variability is essential to improve climate prediction, as well as to give important information to minimize the impact of adverse climate conditions. There are many studies on climate variability over Brazil, attempting to understand its effects on precipitation regimes. For this purpose reliable information on precipitation is required. The lack of reliable information about rainfall over Brazil is due to the absence of a dense rain gauge network, mainly over the Amazon region and central Brazil. Satellite-based sensors provide rainfall information on a global scale, but remote-sensing methods used to estimate rainfall from spaceborne instruments are inexact. Apart from rain gauges, radar is one of the most powerful tools to detect and quantify rainfall. The launch of the Tropical Rainfall Measuring Mission (TRMM) satellite on 27 November 1997 provides a unique opportunity to examine rainfall characteristics in tropics in regions that have low density of observations, such as Amazonia and central Brazil.

TRMM Precipitation Radar (PR) is the first spaceborne radar that was designed to capture a more comprehensive structure of rainfall than any spaceborne sensor did before it. TRMM PR provides information on the three-dimensional structure of rainfall over the tropics and subtropics (Simpson et al., 1998; Kummerow et al., 2000).

The objective of the present study is to validate TRMM PR data over Brazil on a climatic scale. For this purpose we compare TRMM PR mean seasonal rainfall estimates with rain gauge station data from Agência Nacional de Energia Elétrica (ANEEL). We also attempt to investigate the performance of TRMM PR data compared with combined satellite/station data from the Global Precipitation Climatology Project (GPCP) data. First, we investigate the TRMM PR errors compared to ANEEL data for the five geographic Brazilian regions, which are characterized by different precipitation regimes. In a second step we analyze the regional characteristics of the mean seasonal rainfall from TRMM PR and compare with ANEEL and GPCP data. In section 2 we give a brief description of the precipitation data sources used in the study and their inherent errors, and the methodology for the analysis; the regional characteristics of validation are presented in section 3; and section 4 contains the conclusions.

## 2. Data and methodology

### 2a) Data sources

TRMM satellite data are available since December 1997. In the present study we use the accumulated monthly rainfall time series from the TRMM PR-Level 3 (version 5), which is designated as 3A25G2 ([http://helios.eorc.jaxa.jp/pub/TRMM/L3\\_data/Ver/](http://helios.eorc.jaxa.jp/pub/TRMM/L3_data/Ver/)).

These data are available at a high resolution grid ( $0.5^\circ \times 0.5^\circ$ , latitude x longitude). TRMM PR scanning width of about 220 km measures the rainfall rate from the earth surface to 20 km altitude with a horizontal resolution of 4.3 km at nadir and a vertical resolution of 0.25 km (Kummerow et al., 1998). The rainfall rates are calculated from radar reflectivity with corrections for attenuation based on Iuguchi and Meneghini (1994). TRMM PR provides information on the three-dimensional structure of rainfall. Besides the rainfall intensity, TRMM PR also contains information on rain types including stratiform, convective and others. Several papers give a detailed description of TRMM PR products and applications (Adler et al., 2000; Fu and Liu, 2001, 2003; Kummerow et al., 2004; Fu et al., 2003; Zheng et al., 2004).

GPCP data merges precipitation data sets involving measurements of rain gauge from the Global Precipitation Climatology Center (GPCC) (Rudolf, 1993; Rudolf et al., 1994) with various satellite based observations, such as GPI (Arkin and Meisner, 1987), OPI (Xie and Arkin, 1998), SSM/I Emission (Wilheit et al., 1991), SSM/I scattering (Ferraro and Marks, 1995; Ferraro et al., 1996) and TOVS (Susskind et al., 1997). GPCP data are available since 1979. We use the rainfall data obtained from GPCP version 2 (Huffman et al., 1997; Adler, 2003) (<http://lwf.ncdc.noaa.gov/oa/wmo/wdcamet-ncdc.html>). These data are in a  $2.5^\circ \times 2.5^\circ$  latitude x longitude grid.

Rain gauge station data for Brazil from ANEEL are available for the period 1979 to 2000 for a large number of stations (Fig. 1). The data were checked for consistency (deleting unreasonable values from a climatological viewpoint) and are available at <http://hidroweb.aneel.gov.br>). Although there is a dense concentration of stations in the northeast, the data are sparse in the north and central regions of Brazil.

In order to obtain spatial homogeneity, in the present study the values of rainfall obtained from TRMM PR are extrapolated to  $2.5^\circ \times 2.5^\circ$  latitude x longitude intervals and the rainfall data from ANEEL are averaged at each  $2.5^\circ \times 2.5^\circ$  grid. Since ANEEL data are available only up to year 2000 monthly means for the period December 1997 to November 2000 are considered for the three precipitation data sources.

## 2b) Data source errors

Monthly rainfall estimates from TRMM satellite contain errors due to discrete temporal sampling and remote spaceborne rain retrievals. As TRMM satellite is a low earth-orbiting satellite, its rain sensors sample the regional atmosphere only at discrete time intervals. Sampling frequency is a function of latitude, with more samples collected per month at higher latitudes. Monthly estimates are then generated based on the arithmetical mean of the observations collected at the standard gridding resolution. Many studies have shown that the range of temporal sampling errors are about  $\pm 8-12\%$  per month relative to the mean rainfall (Shin and North, 1988; North and Nakamoto; 1989; Bell et al., 1990). The sampling errors in TRMM monthly estimates are associated with the sampling frequency of the satellite and the coverage area of the sensor. In the case of Brazil, the standard deviations (SDs) (for the period 1998-2005) are lesser in the northeast region ( $1-2 \text{ mm h}^{-1}$ ). SD values are around  $2-3 \text{ mm h}^{-1}$  in the central and southeast regions of Brazil, and  $3-4 \text{ mm h}^{-1}$  in Amazonia. The largest values occur in the southern region ( $4-5 \text{ mm h}^{-1}$ ) [http://disc.sci.gsfc.nasa.gov/data/datapool/TRMM\\_DP/01\\_Data\\_Products/02\\_Gridded/02\\_Monthly\\_Pr\\_Prod\\_3A\\_25/](http://disc.sci.gsfc.nasa.gov/data/datapool/TRMM_DP/01_Data_Products/02_Gridded/02_Monthly_Pr_Prod_3A_25/).

TRMM PR and TMI (TRMM Microwave Imager) suffer from regional sampling errors incurred. Since the PR has a narrower swath width (220 km) compared to the TMI (758.5 km) (Kummerow et al., 1998) the expected sampling error is greater (around 30%). However, the TMI retrieval error exceeds retrieval error for PR by about a factor 2 (Fischer, 2007). Due to their larger swath width the use of TMI data generally creates a superior overview of the synoptic rainfall events, but comes at the expense of a decrease in the resolution (Stano et al., 2002). PR produces more reliable estimates of precipitation near the surface than passive microwave does. The use of radar for the measurement of precipitation allows the detection of rain occurring at brightness temperatures greater than those used in passive techniques. Moreover much of the light and heavy rainfall is missed by passive microwave because of its small scale and/or its nature (for example “warm rain”). In both cases PR is more able to measure and quantify the precipitation than TMI (De Angelis et al., 2004).

GPCP precipitation estimates over land are mainly generated by rain gauge. Gridded rain gauge precipitation is subject to systematic errors (losses due to aerodynamic effects), sampling error (due to poor station density) and a methodical error (due to the interpolation method). Intercomparison studies by GPCC revealed that the methodical error is much smaller than the sampling error. It has been found necessary to have at least five gauges in a  $2.5^\circ \times 2.5^\circ$  grid box to reduce sampling errors to within 10% (Legates and Willmott 1990). Details on the sampling error and availability of data are discussed by Rudolf et al. (1994, 1998). In addition to the errors related with rain gauge data there are errors inherent to the satellite based observations. The geosynchronous infrared (IR) based estimates employ the Geostationary Operational Environmental Satellite (GOES) Precipitation Index (GPI; Arkin and Meisner, 1987) technique, which relates cold cloud top

area to rain rate. The OPI technique (Xie and Arkin, 1998) is based on the use of low-Earth-orbit satellite OLR (outgoing longwave radiation) observations. Lower OLR radiances are directly related to higher cloud tops, which are related to increased precipitation rates (Adler et al., 2003). However, non-precipitating high clouds like cirrus also show low values of OLR so that an overestimation of precipitation is expected (Franchito et al., 2008; Marengo et al., 2001). Thus, OLR rainfall derived from precipitation datasets (Xie and Arkin, 1998) includes several false returns from the overhanging cirrus (and related cloud tops) (Fu and Liu, 2003). In the case of Brazil, the largest random errors (which include algorithm and sampling error) for the mean period 1998-2005 occur in Amazonia (higher than  $8 \text{ mm day}^{-1}$ ), where there is a sparse rain gauge distribution, while in the southern and northeast regions, where there is a dense concentration of rain gauge stations, the errors are lesser ( $4\text{-}6 \text{ mm day}^{-1}$ , and less than  $2 \text{ mm day}^{-1}$ , respectively) (<ftp://rsd.gsfc.nasa.gov/pub/gpcpv2cl/>).

Compared to TRMM PR estimates, rain gauges measurements are more or less continuous in time but with very small coverage in area, whereas radar views irregularly shaped volumes of the atmosphere at frequent but noncontinuous intervals of time. As mentioned earlier, rain gauge is subject to systematic errors related to losses due the aerodynamic effects. For example, gauges have a tendency to underestimate rainfall in high winds conditions ([http://radarmet.atmos.colostate.edu/~snesbitt/research/nesbitt\\_jampaper.pdf](http://radarmet.atmos.colostate.edu/~snesbitt/research/nesbitt_jampaper.pdf)).

## 2c) Processing methods

The data coverage for this study is for three years (December 1997-November 2000). The seasonal analyses are based on 3-month averages: December-January-February (DJF), March-April-May (MAJ), June-July-August (JJA) and September-October-November (SON). As mentioned earlier, we concentrate our analyses on the five geographic regions of Brazil: North, Northeast, Central, Southeast and South Regions, as shown in Fig. 1. Tropical rain forest climate lies in the northern region; the northeastern and southern regions are characterized by a semiarid and temperate climate, respectively; savanna and cerrado are found in the central Brazil while the southeastern Brazil is a transition region between semiarid and temperate climates. The ANEEL ground stations are distributed very heterogeneously in the country, as shown in Fig.1. Based on the location of the ANEEL stations and the available rainfall data measured during the period December 1997-November 2000, five areas were chosen inside the five geographic regions ( $R_1$ ,  $R_2$ ,  $R_3$ ,  $R_4$  and  $R_5$  in Fig. 1). The averaged precipitation data series for each  $2.5^\circ \times 2.5^\circ$  grid cell inside these areas are at least 15 months long. For each region, bias (MBE), absolute error and root-mean-square error (rmse) are calculated for TRMM PR and GPCP rainfall estimates. The reference is to ANEEL rain gauge data. The percentage or relative MBE (% MBE), % absolute error and rmse (% rmse) are also calculated for each region. In the analysis, % MBE and % rmse are used to ascertain the systematic and random components of the error, respectively, in the TRMM PR and GPCP data (Adeyewa and Nakamura, 2003). The parameter % rmse is used to evaluate the reliability of each data source in the different regions of Brazil. When the rmse of a rainfall estimate is less than 50% of measured rainfall amount, such estimates are reliable. On other hand, when the rmse is equal to or higher than 50% of the magnitude of the reference rainfall the estimate is considered unreliable for the region and particular season. The errors are calculated only

when the data are available at a particular grid point for all the three data sources. Scattergrams of mean seasonal precipitation of ANEEL rain gauge versus TRMM PR and GPCP rainfall estimates are also plotted for the five Brazilian regions. After computing the bias, absolute error and rmse, we analyze the regional characteristics of the mean seasonal rainfall from TRMM PR and compare with ANEEL and GPCP data.

### 3. Results

#### 3a) Computation of the correlation coefficient, bias, absolute error and rmse

In Figs. 2 and 3 the mean seasonal (DJF and JJA) rainfall from ANEEL are plotted against the rainfall estimates from GPCP and ANEEL, respectively, for the five regions ( $R_1$ ,  $R_2$ ,  $R_3$ ,  $R_4$  and  $R_5$ ) of Fig. 1. In each region GPCP estimates match better the rain gauge data compared with TRMM PR. The best agreements between TRMM PR and ANEEL are obtained for the tropical rain forest ( $R_5$ ) in DJF and for the semiarid ( $R_1$ ) and tropical rain forest ( $R_5$ ) in JJA, and the poorest agreement occurs in the savanna and cerrado regions ( $R_4$ ) for both DJF and JJA. Fig. 4 shows that there is a good agreement between the mean precipitation values and their dispersion around the mean for the three data sources, mainly for DJF and JJA. During MAM, over the region  $R_5$ , and SON, over the region  $R_3$ , the TRMM PR mean and dispersion values are very different from ANEEL and GPCP values. Over the region  $R_5$  the mean precipitation is underestimated, although the dispersion is about the same compared to ANEEL and GPCP, and over the region  $R_3$  the mean and dispersion are overestimated. During SON the TRMM estimates show the mean and dispersion values larger than ANEEL and GPCP values over all the regions, except  $R_1$ .

The correlation coefficients (c.c) between the two precipitation sources (TRMM PR and GPCP) and ANEEL for the each season are showed in Fig. 5a and Table 1. It can be noted that seasonal values of c.c between TRMM PR and ANEEL are high (significant at 99% confidence level by a two sided students' t-test) for most of the regions. The highest values occur in the semiarid region (R<sub>1</sub>) during MAM (89.6%) and JJA (84%) and during DJF and JJA (> 84%) in the tropical rain forest (R<sub>5</sub>). The values of c.c are not significant only in the temperate region (R<sub>3</sub>) during JJA and in the transition region (R<sub>2</sub>) during SON. In the case of GPCP data, the c.c values are higher than in TRMM PR in all the regions, except in the savanna and cerrado region (R<sub>4</sub>) during SON, where they are not significant.

Figure 5b show the seasonal variation of the % MBE for the five regions of Fig. 1 for TRMM PR and GPCP. As can be seen, the % MBE for TRMM PR is negative in most seasons for all regions. Positive % MBE is obtained for the temperate region (R<sub>3</sub>) in JJA and SON, and for the savanna and cerrado (R<sub>4</sub>) and tropical rain forest (R<sub>5</sub>) regions in SON. The absolute value of the % MBE for TRMM PR is in general lower than 25%. The highest value of the % MBE occurs in the temperate region (R<sub>3</sub>) (75%) in SON. Fig. 5b also shows that the % MBE for GPCP is generally positive for almost all the regions. Also, the absolute % MBE is always lower than 25%. The values of % MBE for GPCP is lower in most of the five regions compared with TRMM PR values. However, in the semiarid region (R<sub>1</sub>) in DJF and in the temperate region (R<sub>3</sub>) in DJF and MAM the % MBE values in GPCP are higher than in TRMM PR.

Figure 6a shows the seasonal variation of the relative (%) absolute error for the five regions of Fig. 1 for TRMM PR and GPCP. As can be noted, the % absolute error for TRMM PR is in general lower than 50% in most seasons for all regions. The lowest values

occur in DJF and MAM for the five regions, while the highest values occur in the savanna and cerrado region (R<sub>4</sub>) in JJA and SON and in the temperate region (R<sub>3</sub>) in SON. The % absolute errors for GPCP are always lower than 50% for all the regions. Also, they are lower than in TRMM PR, except for the tropical rain forest region (R<sub>5</sub>) in DJF.

Figure 6b shows the seasonal variation of the % rmse for the five regions of Fig. 1 for TRMM PR and GPCP. As can be seen, the % rmse values for TRMM PR are  $\leq 39\%$  for the all the regions in DJF and MAM. However, in JJA they are higher than 50% in the semiarid (R<sub>1</sub>), transition (R<sub>2</sub>) and savanna and cerrado (R<sub>4</sub>) regions. In SON values of % rmse are also higher than 50% in the semiarid (R<sub>1</sub>), temperate (R<sub>3</sub>) and savanna and cerrado (R<sub>4</sub>) regions. GPCP rainfall estimates show values of % rmse less than 50% for all the regions, except for the semiarid (R<sub>1</sub>) and transition region (R<sub>2</sub>) in JJA.

The mean seasonal values of the c.c, % MBE, % absolute error and % rmse for the five regions of Fig. 1 for TRMM PR and GPCP are summarized in Table1.

The results presented above showed that the seasonal c.c values between TRMM PR and ANEEL rainfall are high (significant at 99% confidence level) in most of the five regions of Fig. 1. The results indicated that the precipitation product of TRMM PR is reliable for the five regions of Fig. 1 in DJF and MAM, since the values of the % rmse and % MBE are low in these areas. In JJA the TRMM PR estimates are only reliable in the temperate (R<sub>3</sub>) and tropical rain forest (R<sub>5</sub>) regions. In the other regions the TRMM PR precipitation product is unreliable because of the inherent error in its estimation generally exceeds 50% of the reference rainfall amount (% rmse > 50%). Thus, one can conclude that the random error is high in these regions during this period. In SON the TRMM PR rainfall estimates are only reliable in the transition region (R<sub>2</sub>) and in the tropical rain forest (R<sub>5</sub>).

Particularly, in the temperate ( $R_3$ ) and savanna and cerrado region ( $R_4$ ) both the % rmse and % MBE are high. It therefore can be concluded that in this season the random and systematic errors are high in these regions. The GPCP precipitation is reliable in the five regions of Fig. 1 during all seasons, except in JJA in the northeastern and southeastern regions. This is due to the fact that the errors were calculated using as reference the ANEEL rainfall. Since GPCP rainfall estimates over land are mainly based on rain gauge data lower errors compared with TRMM PR are expected. However, in the regions with a sparse data coverage GPCP uses satellite products so that errors due to the use of OLR and IR sensors occur, as mentioned earlier. Thus, the results presented in this section regarding GPCP rainfall are valid only for the regions with a dense rain gauge concentration. TRMM PR is subject to random errors, which includes algorithmic and sampling errors. Since TRMM PR uses the same tool to detect and quantify rainfall the reliability of its use over the several regions of Brazil discussed in section 3a is representative.

In the next section we attempt to investigate the characteristics of rainfall over Brazil as a whole, and not only where the rain gauge data are available. For this purpose, we use TRMM PR, GPCP and ANEEL data in a  $2.5^\circ \times 2.5^\circ$  grid covering the entire country, as described in section 2a.

### 3b) Characteristics of rainfall over Brazil in TRMM, ANEEL and GPCP data

In this section we examine the mean seasonal characteristics of rainfall over Brazil comparing the TRMM PR estimates with ANEEL and GPCP precipitation data. Due to the sparsity of rain gauge stations in the Amazonia and central Brazil, the comparison of

TRMM PR rainfall estimates with the ANEEL data is a difficult task. So, the comparison between TRMM PR and GPCP improves the analysis. We concentrate our analysis on the periods DJF and JJA, which corresponds to the rainy and dry seasons of most Brazil (Gan et al., 2005; Rao and Hada, 1990). Figs. 7a-c show the mean rainfall for DJF for TRMM PR, GPCP and ANEEL, respectively. The mean rainfall for JJA is showed in Figs. 7d-f. The differences TRMM PR minus ANEEL, GPCP minus ANEEL and TRMM PR minus GPCP are shown in Fig. 8. As can be seen in Fig. 7a-b, both TRMM PR and GPCP data show in DJF a region of maximum rainfall over central Brazil with northwest to southeast orientation, indicating that they reproduce correctly the strength and orientation of the South Atlantic convergence zone (SACZ). The general pattern distribution of precipitation is similar in TRMM PR, GPCP and ANEEL (Figs. 7a-c). However, there are some differences. The region of high rainfall over northwestern and central Brazil is larger in GPCP than in TRMM PR. Also, the peak of rainfall in ANEEL data is lower (higher than 700 mm) compared with the other two precipitation data (900 mm). A peculiar feature, which is noted in Figs. 7a and 7b, is that in both TRMM PR and GPCP data the high rainfall area extends towards the north-northeast of Brazil (10°S, 50°W). Over these region a center of maximum rainfall of about 700 mm is seen in TRMM PR, while in GPCP data the rainfall is stronger (around 900 mm). This is not seen in ANEEL data. Fig. 8a shows that the higher positive differences TRMM PR minus ANEEL ( $\geq 100$  mm) occur in the southwestern and eastern Amazonia and in the central Brazil. This region of positive differences is larger in the case of GPCP data, extending from the western Amazonia to the northeastern Brazil (Fig. 8b). Also, the positive differences are higher in GPCP compared with TRMM PR. Fig. 8c shows that the precipitation in TRMM PR is less than in GPCP

over most of Brazil, except in a small area of the southern region. The highest negative differences TRMM PR minus GPCP ( $\geq 100$  mm) are found in the northeastern Amazonia and in the central Brazil. As shown in section 3a, the TRMM PR random and systematic errors are low in these regions in DJF. Due to the sparsity of rain gauge data in these regions, we suggest that these high negative differences are due mainly to the use of the satellite observations in GPCP. As mentioned earlier, satellite observations based on IR and OLR sensors contribute to an overestimation of convective rainfall due to the presence of high cirrus cloud. Since strong convective rainfall dominates over Amazonia and central Brazil, an overestimation of the precipitation leads to an increase of the negative differences TRMM minus GPCP estimates in DJF in these regions. Because of TRMM PR is better at taking into account the vertical structure of the rain systems (Adler et al., 2000), it is able to capture convective rainfall areas. Thus, in these regions the TRMM PR rainfall estimates are more reliable than in GPCP. This is in agreement with the higher random errors in GPCP over Amazonia compared with the other Brazilian regions (section 2b).

Figures 7d-f show that both TRMM PR and GPCP reproduce well the dry season over most of Brazil during JJA and the high rainfall over the northwestern Amazonia, the eastern coast and the southern parts of Brazil, in agreement with ANEEL rainfall. However, there are some quantitative differences. TRMM PR and GPCP estimates are less than ANEEL rainfall over the northeast coast of Brazil (Figs. 8d-f). The negative differences (TRMM PR minus ANEEL and GPCP minus ANEEL) are due to the high random errors in TRMM PR and GPCP estimates in JJA in the northeastern region, as discussed in section 3a. Although the two data sources are unreliable in this region during JJA, TRMM PR estimates are less than GPCP estimates. Over the southern region TRMM PR rainfall

exceeds ANEEL and GPCP rainfall. Although both TRMM PR and GPCP data are reliable in this region, GPCP is in better agreement with ANEEL data. This is due to the fact the % rmse in TRMM PR is higher (42.8%) than in GPCP (19.8%) (Fig. 6b and Table 1). From Figs. 8e and 8f it can be noted that GPCP rainfall exceeds ANEEL and TRMM PR rainfall in some parts of Amazonia due to the overestimation of the convective rainfall by GPCP in this region.

The analysis of the mean characteristics of rainfall over Brazil were based on the periods DJF and JJA, which correspond to the rainy and dry season for most of Brazil. Analysis of the rainfall for the transition seasons indicate that both TRMM PR and GPCP reproduce the high rainfall during the rainy season (MAM) over the north-northeast Brazil and the maximum rainfall over the southern Brazil in SON (figures not shown). MAM is the rainfall season for the drought prone northeast Brazil and a reliable rainfall estimation is necessary to monitor drought situation. Again, TRMM PR rainfall is less than GPCP rainfall over the north-northeast Brazil and TRMM PR estimates greatly exceed GPCP estimates over the southern Brazil. Although TRMM PR precipitation data are reliable over the northeast Brazil in MAM the % rmse values in TRMM PR are higher (42.3%) compared with those in GPCP (29.5%), as shown in Fig. 6b and Table 1. This seems the cause for the negative differences TRMM PR minus GPCP in the region. The reason for the high positive differences TRMM PR minus GPCP over the southern Brazil in SON is attributed to the fact TRMM PR data are not reliable in this season in this region.

#### 4. Conclusions

In this study the potentialities and limitations of TRMM PR data over Brazil were evaluated comparing the characteristics in these data with rain gauge station data from ANEEL and combined satellite/station data from GPCP. The precipitation data in a  $2.5^\circ \times 2.5^\circ$  grid for a 3-yr period (December 1997-November 2000) were used. The analysis was conducted on a seasonal basis and considered five Brazilian geographic regions, which have different climatic characteristics and precipitation regimes. First the c.c, bias, absolute errors and rmse were computed for TRMM PR and GPCP with respect to ANEEL rain gauge data. Latter, the regional characteristics of the mean seasonal rainfall over Brazil from TRMM PR were examined and compared with ANEEL and GPCP data.

The results showed that the TRMM PR seasonal rainfall is well correlated with ANEEL rainfall (c.c significant at 99% confidence level by a two sided student t-test) in most of the five regions. However, the random and systematic errors are sensitive to seasonal and regional differences. During DJF and MAM the precipitation product of TRMM PR is reliable for the five regions of Brazil. In JJA the TRMM PR estimates are only reliable in the Amazonian and southern regions. In the other regions the TRMM PR precipitation product is unreliable because the inherent error in its estimation generally exceeds 50% of the reference rainfall amount (% rmse > 50%). Thus, one can conclude that the random error is high in these regions during this period. During SON the TRMM PR rainfall estimates are only reliable in the Amazonian and southeastern regions. In the particular cases of the southern and central regions the random and systematic errors are high in these regions. The GPCP precipitation product is reliable in most of the five regions during all seasons, except in JJA in the northeastern and southeastern regions. The better agreement between GPCP and ANEEL is due to the fact that GPCP rainfall estimates over

land are mainly based on rain gauge data. However, in the regions with a sparse data coverage GPCP uses satellite products so that error inherent to the use of OLR and IR sensors occur.

Regarding the mean seasonal rainfall characteristics over Brazil in general the TRMM PR estimates in DJF are in good agreement with ANEEL and GPCP data. The highest positive differences TRMM PR minus ANEEL occur in the southwestern and eastern Amazonia and in the central Brazil. The precipitation in TRMM PR is less than in GPCP over most of Brazil. The highest negative differences TRMM PR minus GPCP are found in the northeastern Amazonia and in the central Brazil. The TRMM PR random and systematic errors are low in these regions in DJF. We suggest that the high negative differences are due mainly to an overestimation of convective rainfall (because the presence of high cirrus cloud) by the IR and OLR sensors in GPCP. This is in agreement with the higher random errors in GPCP over Amazonia compared with the other Brazilian regions. TRMM PR reproduces well the dry season over most of Brazil during JJA in agreement with ANEEL and GPCP data. However, TRMM PR and GPCP estimates are less than ANEEL rainfall over the northeast coast of Brazil. This is due to the high random errors in TRMM PR and GPCP estimates in this season. Over the southern region TRMM PR rainfall exceeds ANEEL and GPCP rainfall. The positive differences in the southern Brazil are attributed to the higher % rmse in TRMM PR than in GPCP, although TRMM PR estimates are reliable in JJA over this region. In general, for most seasons TRMM PR is more reliable than GPCP in the regions with sparse data coverage, while the use of GPCP is more adequate in the regions of a dense concentration of rain gauge stations.

*Acknowledgments:* The third author was supported by Fundação de Amparo à Pesquisa do Estado de São Paulo (FAPESP).

## References

- Adeyewa, Z. D., and K. Nakamura, 2003: Validation of TRMM radar rainfall data over the major climatic regions in Africa. *J. Appl. Meteor. Climatol.*, 42, 331-347.
- Adler, R. F., G. J. Huffman, D. T. Bolvin, S. Curtis, and E. J. Nelkin, 2000: Tropical rainfall distribution determined using TRMM combined with other satellite and rain gauge information. *J. Appl. Meteor.*, 39, 2007– 2023.
- Adler, R. F., and Coauthors, 2003: The Version-2 Global Precipitation Climatology Project (GPCP) monthly precipitation analysis (1979–present). *J. Hydrometeor.*, 4, 1147–1167.
- Arkin, P. A., and B. N. Meisner, 1987: The relationship between large-scale convective rainfall and cold cloud over the Western Hemisphere during 1982–84. *Mon. Wea. Rev.*, 115, 51–74.
- Bell, T. L., A. Abdullah, R. L. Martin, and G. North, 1990: Sampling errors for satellite-derived tropical rainfall: Monte Carlo study using a space–time stochastic model. *J. Geophys. Res.*, 95, 2195–2205.
- De Angelis, C. F., G. R. McGregor, and C. Kidd, 2004: A 3 year climatology of rainfall characteristics over tropical and subtropical South America based on Tropical Rainfall Measuring Mission precipitation radar data. *Int. J. Climatol.*, 24, 385-399.
- Ferraro, R., and G. Marks, 1995: The development of SSM/I rainrate retrieval algorithm using groundbased radar measurements. *J. Atmos. Oceanic. Technol.*, 12, 755–770.
- Ferraro, R., F. Weng, N. C. Grody, and A. Basist, 1996: An eight-year (1987–1994) time series of rainfall, clouds, water vapor, snow cover, and sea ice derived from SSM/I measurements. *Bull. Amer. Meteor. Soc.*, 77, 891–905.

- Fisher, B. L., 2007: Statistical Error Decomposition of Regional-Scale Climatological Precipitation Estimates from the Tropical Rainfall Measuring Mission (TRMM). *J. Appl. Meteor. Climatol.*, 46, 791-813.
- Franchito, S. H., V. B. Rao, P. R. B. Barbieri, and C. M. E. Santo, 2008: Rainy season duration estimated from OLR versus rain gauge data and the 2001 drought in Southeast Brazil. *J. Appl. Meteor. Climatol.* 47, 1493-1499.
- Fu, Y., and G. Liu. 2001: The variability of tropical precipitation profiles and its impact on microwave brightness temperatures as inferred from TRMM data. *J. Appl. Meteor.*, 40, 2130–2143.
- Fu, Y., and G. Liu, 2003: Precipitation characteristics in mid-latitude East Asia as observed by TRMM PR and TMI. *J. Meteor. Soc. Japan*, 81, 1351–1367.
- Fu, Y., Y. H. Lin, G. Liu, and Q. Wang. 2003: Seasonal characteristics of precipitation in 1998 over East Asia as derived from TRMM PR. *Adv. Atmos. Sci.*, 20, 511–529.
- Gan, M. A., V. B. Rao, and M. C. L. Moscati, 2005: South American monsoon indices. *Atmos. Sci. Lett.*, DOI: 10.1002/asl.119.
- Hastenrath, S. Climate Dynamics of the Tropics, 1991. Kluwer, Dordrecht, 488 pp.
- Iguchi, Toshio, and Robert Meneghini, 1994: Intercomparison of single-frequency methods for retrieving a vertical rain profile from airborne or space radar data. *J. Atmos. Oceanic Technol.*, 11, 1507–1516
- Kummerow, C., W. Barnes, T. Kozu, J. Shiue, and J. Simpson, 1998: The Tropical Rainfall Measuring Mission (TRMM) sensor package. *J. Atmos. Oceanic Technol.*, 15, 809–817.
- Kummerow, C., and Coauthors, 2000: The status of the Tropical Rainfall Measuring Mission (TRMM) after two years in orbit. *J. Appl. Meteor.*, 1965–1982.

- Kummerow, C., P. Poyner, W. Berg, and J. Thomas-Stahle, 2004: The effects of rainfall inhomogeneity on climate variability of rainfall estimated from passive microwave sensors. *J. Atmos. Oceanic Technol.*, 21, 624–638.
- Legates, D. R., and C. J. Willmott, 1990: Mean seasonal and spatial variability in gauge corrected, global precipitation. *Int. J. Climatol.*, 10, 111–127.
- Li, R., and FU, Y., 2005: Tropical Precipitation Estimated by GPCP and TRMM PR Observations. *Adv. Atmos. Sci.*, 22, 852-864.
- Huffman, G. J., R. F. Adler, P. A. Arkin, et al., 1997: The Global precipitation climatology project. *Bull. Amer. Soc.*, 78, 5-20.
- Marengo, J., B. Liebmann, V. E. Kousky, N. Filizola, and I. Wainer, 2001: On the onset and end of the rainy season in the Brazilian Amazon Basin., *J. Climate*, 14, 833-852.
- North, G. R., and S. Nakamoto, 1989: Formalism for comparing rain estimation designs. *J. Atmos. Oceanic Technol.*, 6, 985–992.
- Pisciottano, G. F., A. F. Diaz, G. Cazes, and C. R. Mechoso, 1994: El Niño-Southern Oscillation impact on rainfall in Uruguay. *J. Climate*, 7, 1286-1302.
- Rao, V. B., and K. Hada, 1990: Characteristics of rainfall over Brazil: Annual variations and connections with the Southern Oscillation. *Theor. Appl. Climatol.*, 42, 81-91.
- Ratisbona, C. R., 1976: *The climate of Brazil*. Climates of Central and South America. *World Survey of Climatology*, Vol. 12, (W. Schwerdtfeger and H. E. Landsberg, eds), Amsterdam; Elsevier, 219-293.
- Rudolf, B., 1993: Management and analysis of precipitation on a routine basis. *Proc. Int. WMO/IAHS/ETH/SYMP. On Precipitation and Evaporation*, Slovak Hydrometeorology Institute, Bratislava, 69–76.

Rudolf, B., H. Hauschild, W. Rueth and U. Schneider, 1994: Terrestrial precipitation analysis: Operational method and required density of point measurements. *Global Precipitations and Climate Change*, M. Desbois and F. Desalmond, Eds., NATO ASI Series I, 26, Springer-Verlag, 173–186.

Rudolf, B., T. Fuchs, W. Rueth, and U. Schneider, 1998: Precipitation data for verification of NWP model re-analyses: The accuracy of observational results. *Proc. WCRP International Conference on Reanalyses*, Washington, DC, 27-31 Oct 1997, WMO/TD-No. 876, WCRP-104, 215-218.

Stano, G, T. N. Krishnamurti, , T. S. V. Vijaykumar, and A. Chakraborty, 2002: Hydrometeor structure of a composite monsoon depression using the TRMM radar. *Tellus*, 54A, 370-381.

Simpson, J., R. F. Adler, and G. R. North, 1998: A proposed Tropical Rainfall Measuring Mission (TRMM) satellite. *Bull. Amer. Meteor. Soc.*, 69, 278–295.

Shin, K., and G. R. North, 1988: Sampling error study for rainfall estimate by satellite using a stochastic model. *J. Appl. Meteor.*, 27, 1218–1231.

Sussikind, J., P. Piraino, and L. Rokke, T. Iredell, and A. Mehta, 1997: Characteristics of the TOVS pathfinder path A dataset. *Bull. Amer. Meteor. Soc.*, 78, 1449–1472.

Trewartha, G. T., 1961: *The Earth's problem climates*. University of Wisconsin Press, 334 pp.

Wilheit, T. J., A. T. C. Chang, and L. S. Chiu, 1991: Retrieval of monthly rainfall indices from microwave radiometric measurements using probability distribution functions. *J. Atmos. Oceanic Technol.*, 8, 118–136.

Xie, P. P., and P. A. Arkin, 1998: Global monthly precipitation estimates from satellite observed outgoing longwave radiation. *J. Climate*, 11, 137–164.

Zheng Yuanyuan, Fu Yunfei, Liu Yong, Zhu Hongfei, Xie Yifeng, Yao Xiuping, and Yu Rucong, 2004: Heavy rainfall structures and lightning activities in a cold front cyclone happened in Huai river derived from TRMM PR and LIS observations. *Acta Meteorologica Sinica*, 62, 790–802.

months	region	NP	correlation value %		relative root mean square error %		relative mean bias error %		relative mean absolute error %	
			GPCP	TRMM	GPCP	TRMM	GPCP	TRMM	GPCP	TRMM
DJF	R1	60	90.2	74.8	30.5	39.4	16.3	1.6	22.8	31.2
	R2	46	91.2	61.6	13.2	31.5	-1.3	-8.9	9.3	25.2
	R3	21	92.0	76.3	17.4	31.2	9.1	-5.4	14.5	26.0
	R4	34	78.6	47.8	17.3	31.1	2.9	-9.9	13.3	24.7
	R5	32	86.1	84.8	29.9	31.9	0.0	-7.2	23.4	22.1
MAM	R1	60	96.5	89.6	29.5	42.3	14.0	-19.8	21.5	30.6
	R2	45	82.1	61.1	19.7	37.8	-1.7	-10.7	13.7	28.1
	R3	19	91.6	48.0	14.7	36.2	6.8	-4.5	11.6	29.4
	R4	31	55.4	41.8	21.3	36.8	2.6	1.1	17.7	28.0
	R5	31	78.2	36.7	16.0	36.7	-3.2	-25.2	13.1	29.1
JJA	R1	59	88.7	84.0	68.0	104.8	14.7	-47.8	47.4	55.6
	R2	43	86.2	60.6	49.8	79.8	7.8	-13.6	35.5	51.8
	R3	19	73.6	45.3	19.8	42.8	5.3	17.0	16.2	36.3
	R4	26	89.8	39.1	47.9	106.5	9.2	-10.4	32.6	75.4
	R5	32	92.9	84.6	17.4	23.8	3.8	-0.6	14.2	19.7
SON	R1	59	93.5	75.7	26.2	54.8	-3.7	-5.9	20.7	39.0
	R2	43	58.5	15.6	21.0	44.2	-0.6	0.5	13.9	34.7
	R3	19	90.6	80.9	16.0	118.1	-2.5	75.4	14.0	87.3
	R4	26	25.1	47.0	29.8	64.5	9.6	44.3	21.2	52.6
	R5	32	74.6	49.0	20.2	40.6	8.0	16.4	15.9	34.6

Table 1

### Table legends

Table 1: Mean seasonal values of the c.c, % MBE, % absolute error and % rmse for the five regions of Brazil (Fig. 1) for TRMM PR and GPCP compared to the ANEEL. The light (dark) shaded cells represent the region and period where the c.c is not significant at 99% (95%) confidence level by a two sided students' t-test. Also shown is the number of data points in each region.

### Figure legends

Fig. 1: Distribution of the ANEEL stations over the five geographic regions of Brazil. The dashed lines represent the contours of the five selected regions where the 2.5°x2.5° ANEEL precipitation data series for the period December 1997 to November 2000 are at least 15 months long.

Fig. 2: Mean seasonal (DJF) rainfall from ANEEL versus the rainfall estimates from GPCP and ANEEL for the five regions of Fig. 1.

Fig. 3: Same as Fig. 2, but for JJA.

Fig. 4: Dispersion intervals of the mean three months precipitation over regions R<sub>1</sub>, R<sub>2</sub>, R<sub>3</sub>, R<sub>4</sub> and R<sub>5</sub> for the period from Dec 1997 to Nov 2000. The intervals around the mean value are from minus to plus one standard deviation (mean  $\pm$  one standard deviation). The white small rectangle represents the mean value of the three months precipitation.

Fig. 5: Seasonal variations of: a) correlation coefficient obtained between the two rainfall estimates: TRMM PR (slashed bar) and GPCP (grayed bar) and ANEEL rain gauge data, b) % MBE for TRMM PR and GPCP data for the five regions of Fig. 1.

Fig. 6: Seasonal variations of the: a) % absolute error, b) % rmse for TRMM and GPCP data for the five regions of Fig. 1. Legend similar to Fig. 5.

Fig. 7: Mean annual precipitation (mm) (1998-2000) for DJF: a) TRMM PR, b) GPCP, c) ANEEL; d), e), and f): the same as a), b), and c), but for JJA.

Fig. 8: Differences: a) TRMM PR minus ANEEL, b) GPCP minus ANEEL, and c) TRMM PR minus GPCP for DJF; d), e), and f): the same as a), b), and c), but for JJA.

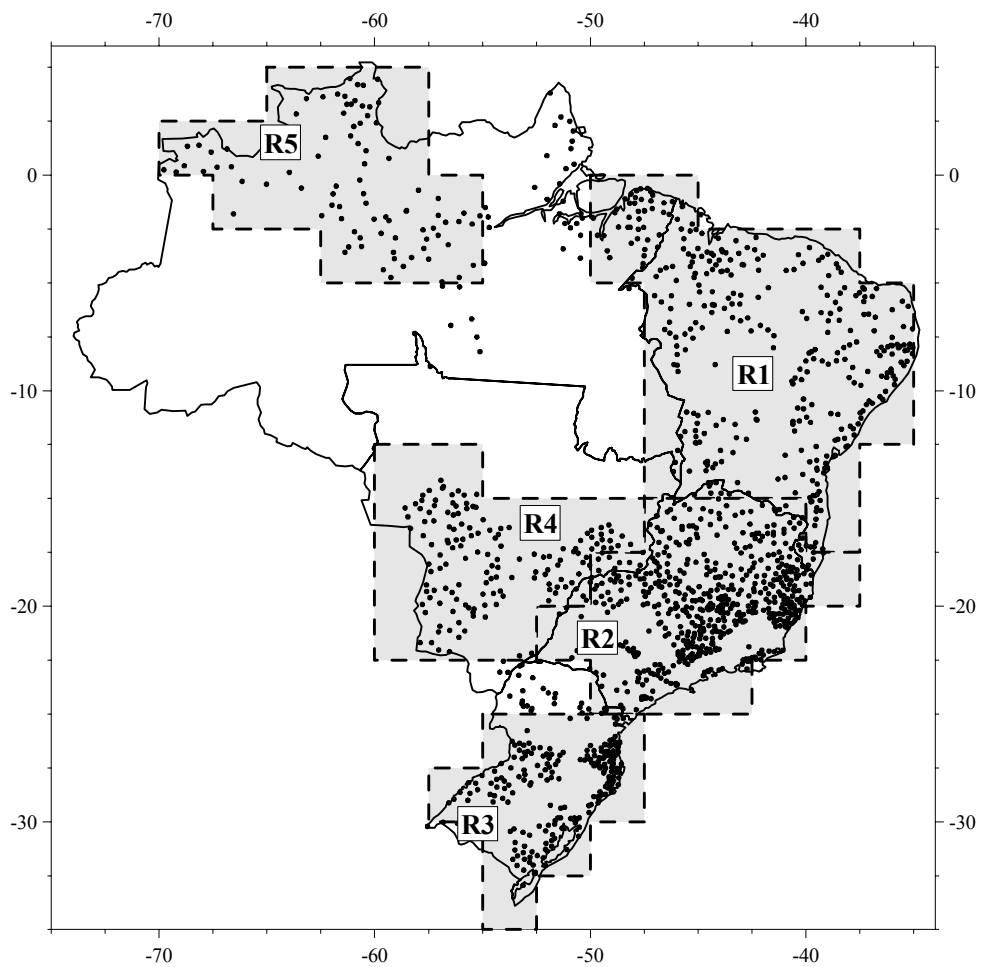


Fig. 1

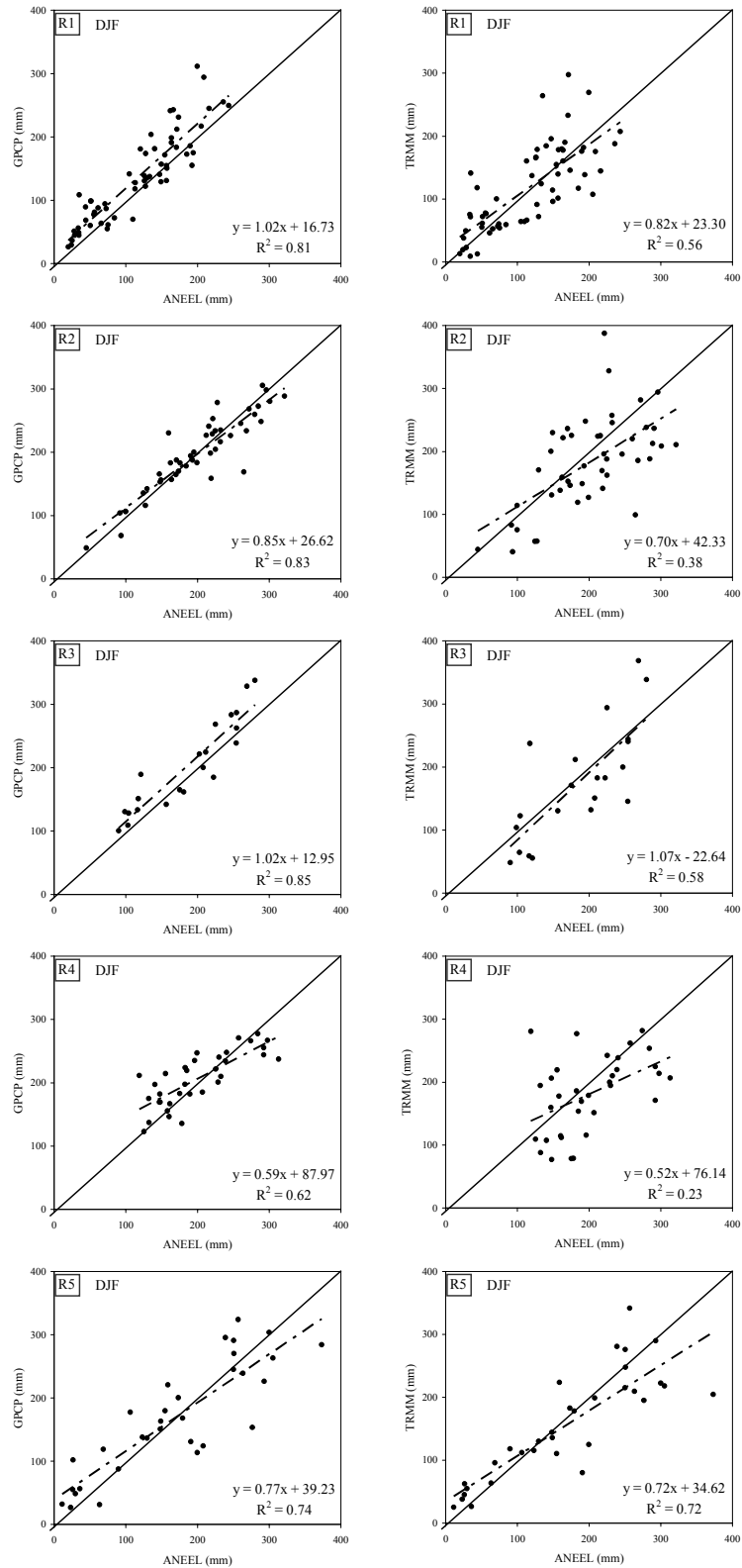


Fig. 2

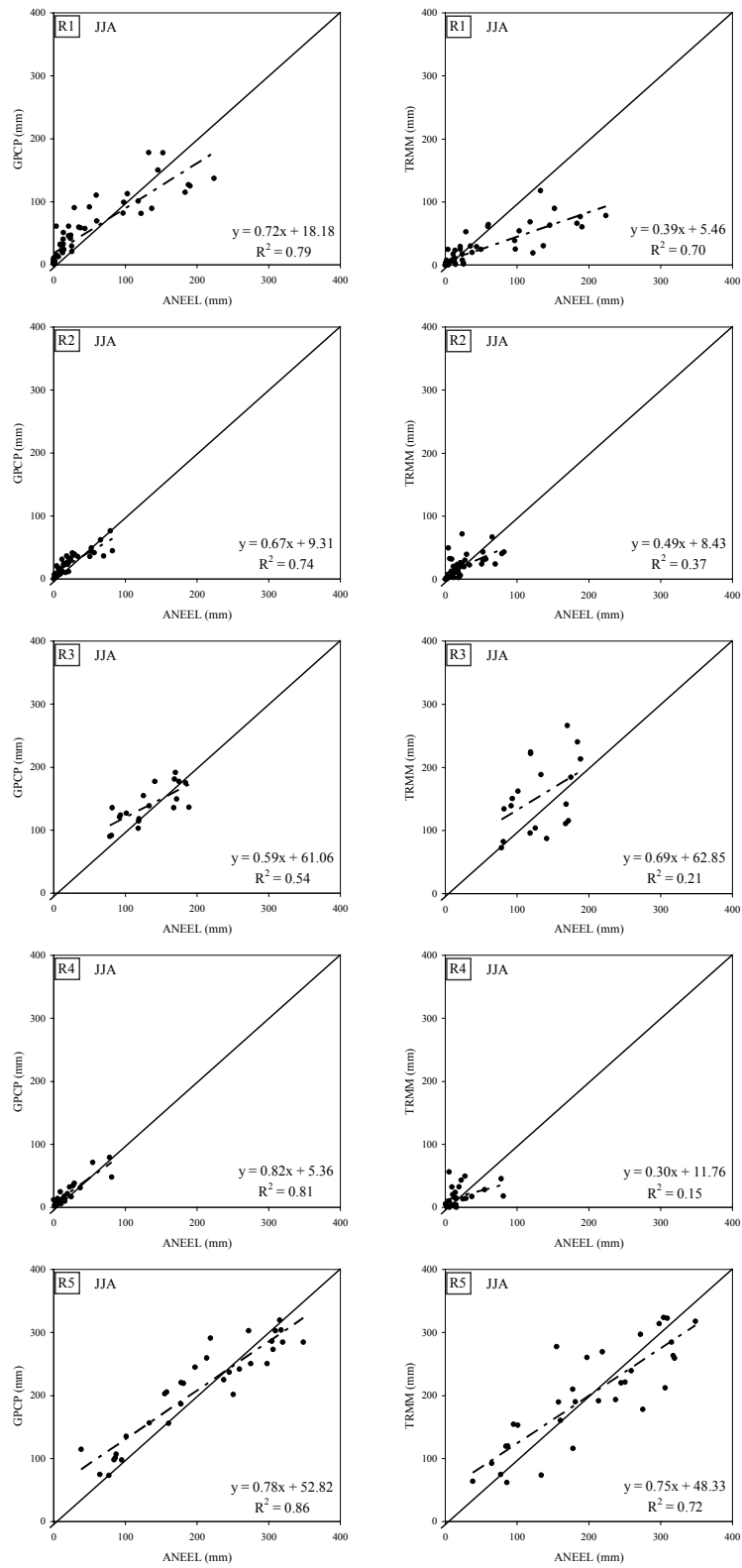


Fig. 3

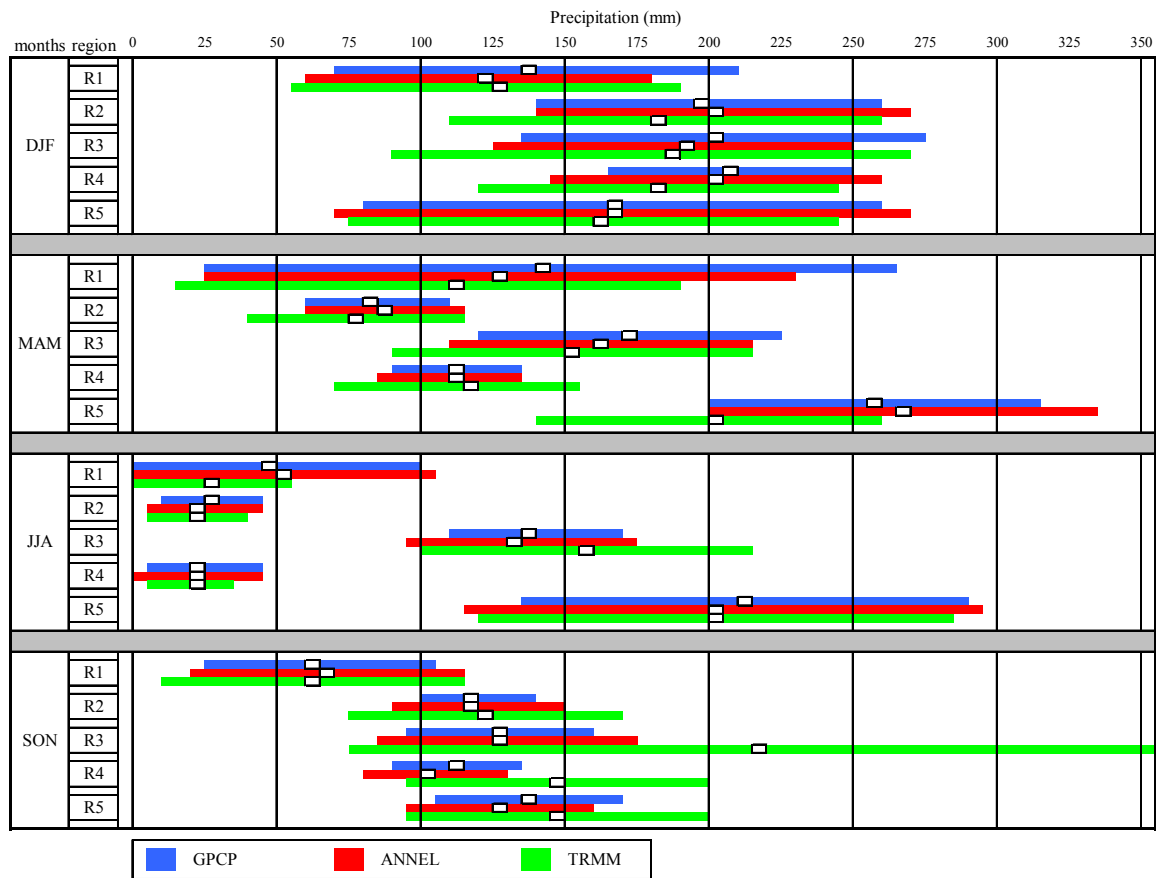


Fig. 4

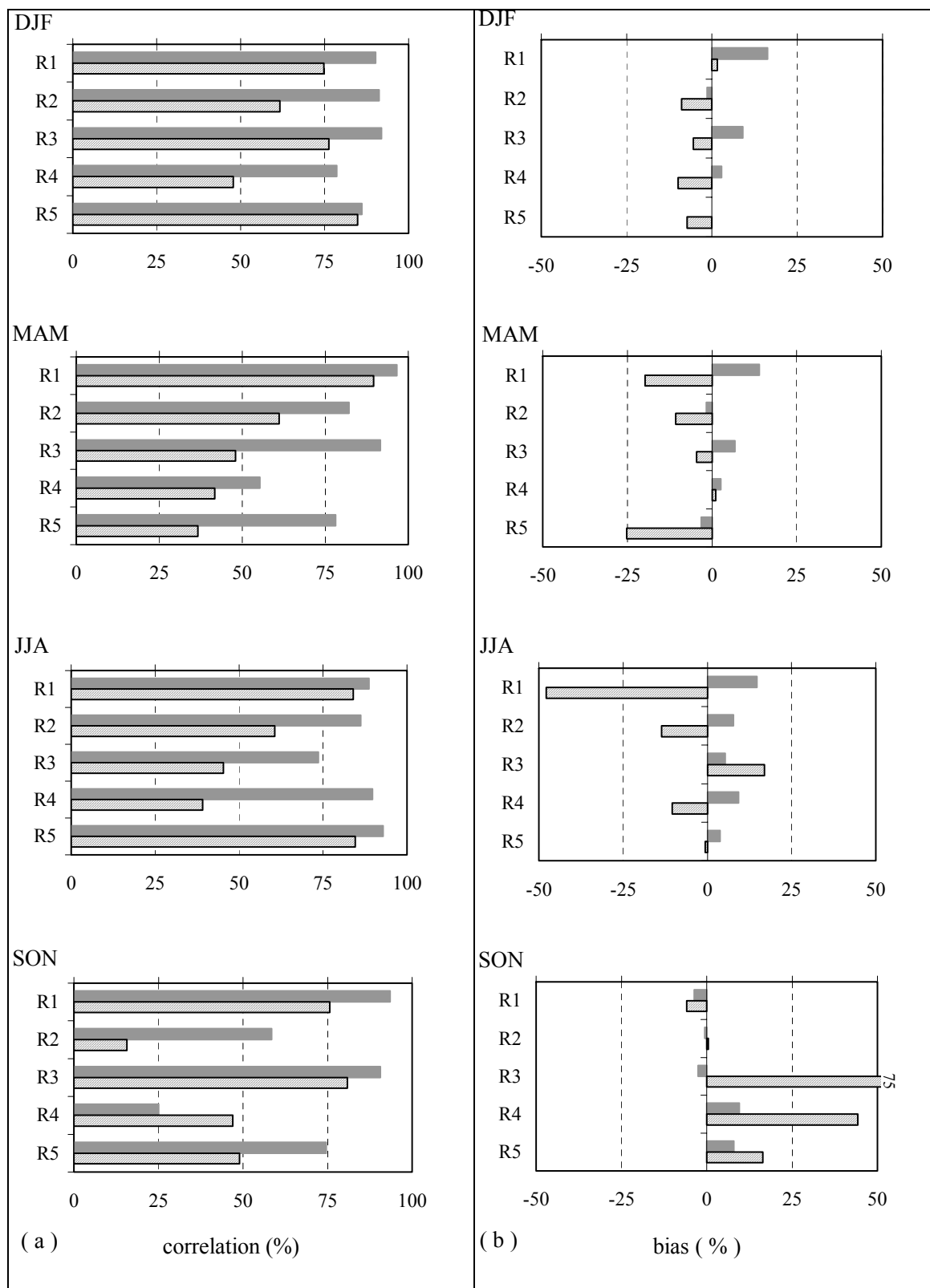


Fig. 5

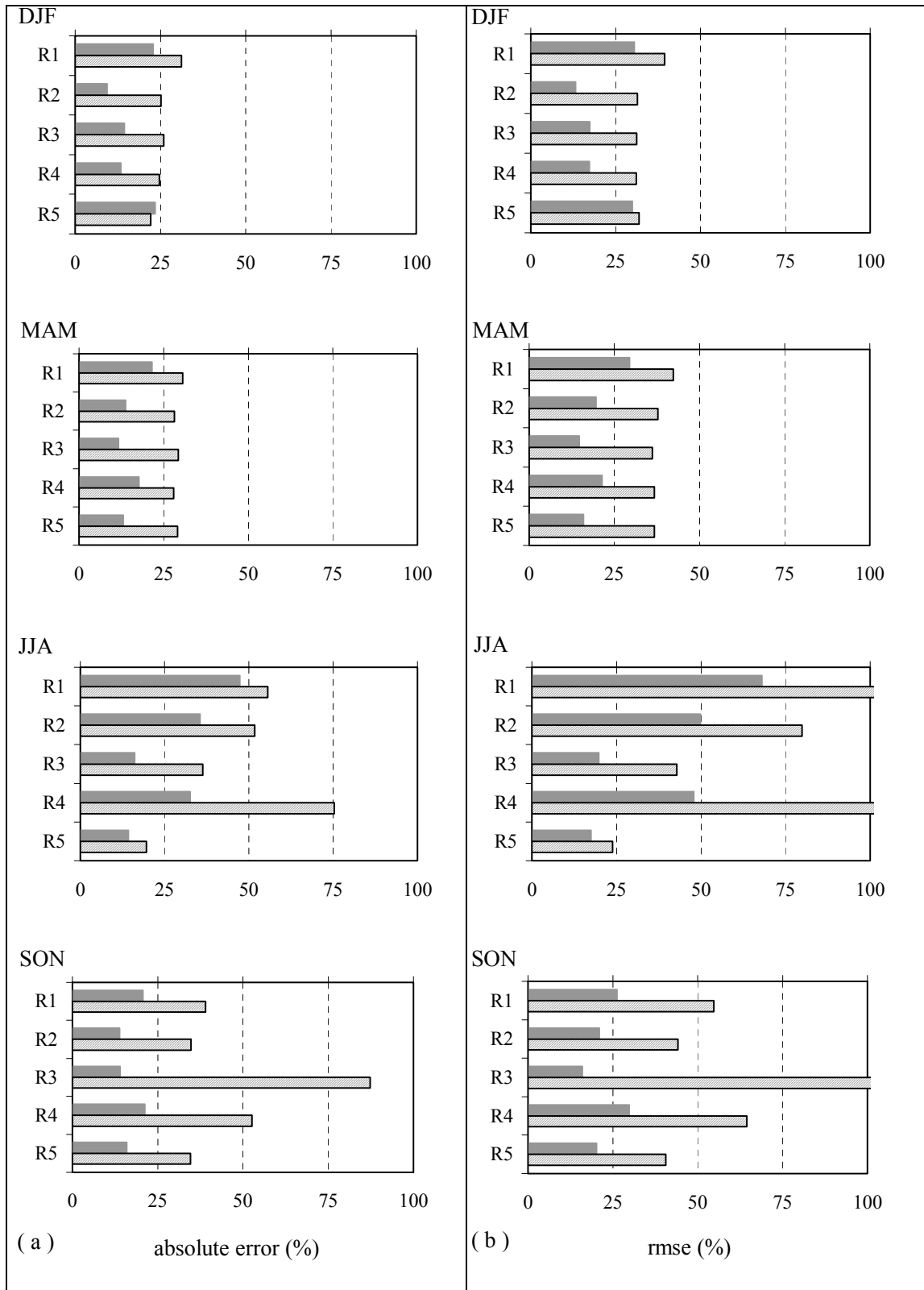


Fig. 6

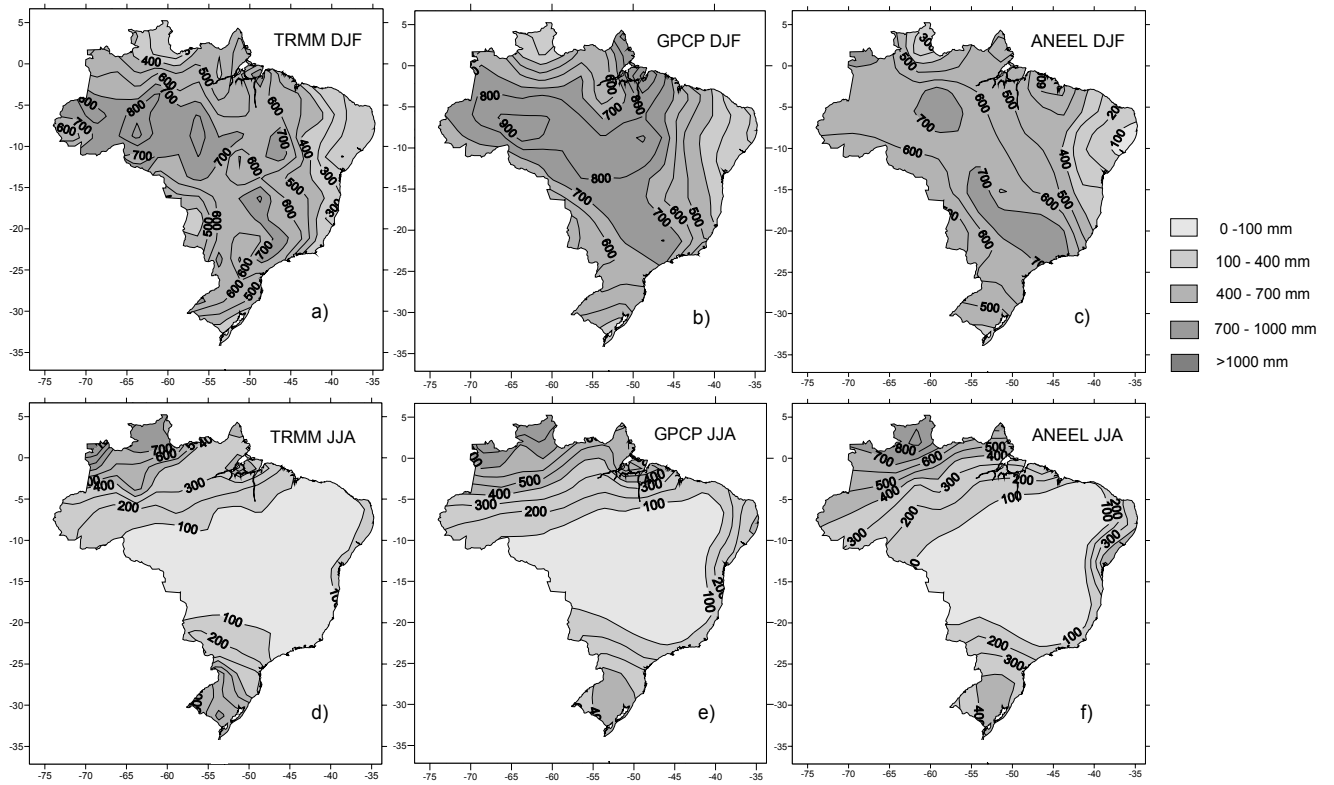


Fig. 7

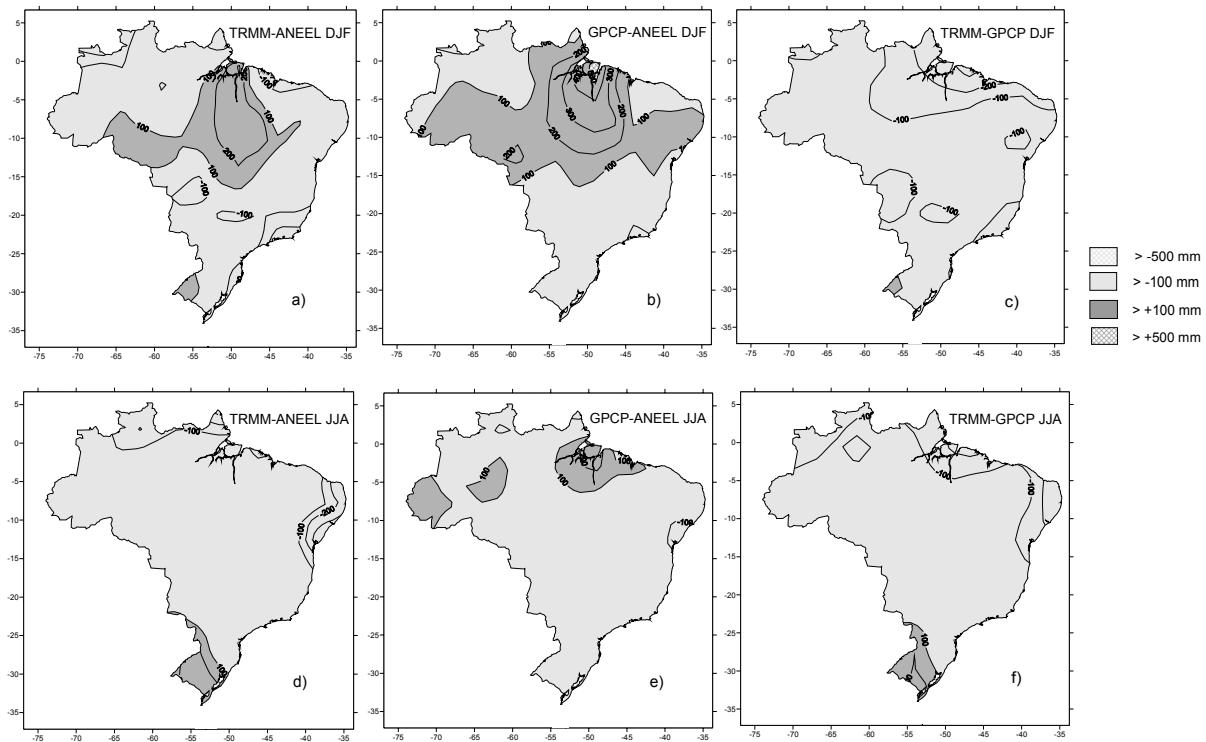


Fig. 8